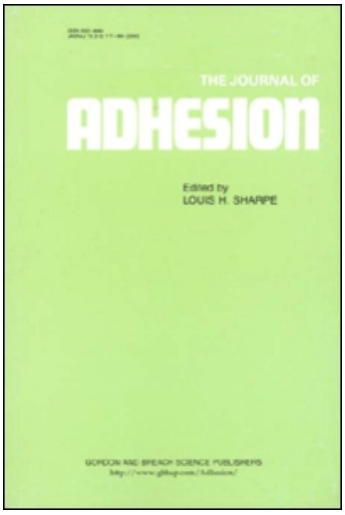

The Journal of Adhesion
Publication details, including instructions for authors and subscription information:
http://www.informaworld.com/smpp/title~content=t713453635

Strengthening the Junction Between EPDM and Aluminium Substrate via Plasma Polymerisation

Vincent Roucoules[a]; Frédéric Siffer[a]; Arnaud Ponche[a]; Unai Egurrola[a]; Marie-France Vallat[a]
[a] Institut de Chimie des Surfaces et Interfaces and Université de Haute-Alsace, Mulhouse Cedex, France

To cite this Article Roucoules, Vincent , Siffer, Frédéric , Ponche, Arnaud , Egurrola, Unai and Vallat, Marie-France(2007) 'Strengthening the Junction Between EPDM and Aluminium Substrate via Plasma Polymerisation', The Journal of Adhesion, 83: 10, 875 — 895
To link to this Article: DOI: 10.1080/00218460701699732
URL: http://dx.doi.org/10.1080/00218460701699732

The Journal of Adhesion, 83:875–895, 2007

ISSN: 0021-8464 print/1545-5823 online
DOI: 10.1080/00218460701699732

Taylor & Francis
Taylor & Francis Group

Strengthening the Junction Between EPDM and Aluminium Substrate via Plasma Polymerisation

Vincent Roucoules
Frédéric Siffer
Arnaud Ponche
Unai Egurrola
Marie-France Vallat
Institut de Chimie des Surfaces et Interfaces and Université de Haute-Alsace, Mulhouse Cedex, France

High interfacial strengths of elastomer to metal joints imply the formation of covalent bonds at the interface. It is proposed to deposit a plasma polymer coating containing double bonds on an aluminium substrate for the formation of cross-links between the elastomer and the coating during peroxide crosslinking of the elastomer. Ethylene-co-propylene-co-diene terpolymer (EPDM) is considered here. Maleic anhydride is polymerised and reacted with allylamine to lead to an amide functionalised plasma polymer which is heated to produce imide functional groups. Plasma polymer coated aluminium/EPDM joints were evaluated by a peel test and the locus of failure was identified by several techniques: SEM, infrared spectroscopy, wettability, and XPS.

Keywords: Adhesion; Crosslinking; Elastomers; Interfaces; Plasma polymerisation

1. INTRODUCTION

Interdiffusion of polymer chains at an interface in order to strengthen it is an important contributing mechanism, although only a portion of long connector chains can be active as shown, for example, by Deruelle *et al.* [1]. The question of the influence of rate of crack opening on the

Received 14 March 2007; in final form 30 July 2007.
One of a Collection of papers honoring Liliane Léger, the recipient in February 2007 of *The Adhesion Society Award for Excellence in Adhesion Science, Sponsored by 3M*.
Address correspondence to Marie-France Vallat, Institut de Chimie des Surfaces et Interfaces (CNRS-UPR 9069), and Université de Haute-Alsace, 15, rue Jean Starcky, B.P. 2488, F-68057 Mulhouse Cedex, France. E-mail: marie-france.vallat@uha.fr

interfacial strength needs to be considered. Indeed, chain entanglements become efficient at high separation rates whereas disentanglements can contribute at very low rates. If intimate contact establishment and chain interdiffusion are the main mechanisms in joint formation of elastomers which are crosslinked into contact, chemical bond formation between interpenetrated chains from each side of the interface is essential. Aradian *et al.* [2] studied the competition of interdiffusion and crosslinking mechanisms and showed that the control parameter depends on the reactivity of the crosslinker, the concentration of reactive sites on the polymer chains, the polymerisation index, and the number of segments between entanglements. However, no quantitative results were given.

One of the most convincing studies done on the relationship between the number of covalent bonds on a polymer interface and the experimental work of adhesion remains the one by Gent and Ahagon [3]. They have shown that the peel strength of a peroxide crosslinked polybutadiene elastomer to a glass substrate treated with a silane solution is directly proportional to the amount of vinyl silane in a solution containing ethyl and vinyl silanes. These functional groups are able to react during peroxide crosslinking of the polybutadiene chains although the direct measurement of the number of covalent bonds created at the interface was never done. It is recognized that covalent bonding is compulsory in getting high interfacial strength in elastomer/metal joining which is generally obtained through the use of primer/adhesive system. The functional groups of the primer are involved in covalent or ionic bonds with the metal surface on the one hand and with the adhesive on the other hand. The adhesive is the link between the primer and the elastomer formulation. Both interdiffusion mechanism and covalent bonding are involved in order to get these strong bonds. The formulation of the adhesive systems is complex and uses solvents which have to be eliminated for more friendly environmental processing. Aqueous based formulations are very often not as efficient.

Therefore, the replacement of this bi-components system by a plasma polymer would simplify the process. Some chain interdiffusion may be expected although plasma polymers are quite tight polymer networks. Moreover, the choice of various reactive functional groups is possible in order to get covalent bonds with the elastomer during crosslinking. Plasma polymer thin coatings are generally recognized as well adhering coatings to all substrates which can improve corrosion resistance of metals as well as adhesive performance [4–8]. The deposition of the plasma thin coating is a clean process without any solvent. Due to tyre applications, great attention was given to the use of plasma

polymers to replace brass coating of steel cords [9,10] or to improve adhesion strength of textile cords to rubber [11,12]. Acetylene, butadiene, and thiophene were considered for increasing adhesion of natural rubber crosslinked by the usual sulphur-based system.

Increase of adhesion of diene rubber crosslinked by peroxide to aluminium substrate *via* plasma polymerisation was never reported.

Ethylene-co-propylene-co-diene terpolymer (EPDM) is known for its poor adhesion to many substrates. The objective of this work is to produce thin coatings which are able to react during the crosslinking procedure of the elastomer. In this study, we considered the possibility of increasing adhesive performance between aluminium substrate and EPDM crosslinked into contact by creating a plasma polymer layer containing double bonds on the aluminium substrate before assembly; these double bonds are able to react during peroxide crosslinking of EPDM. Indeed, maleic anhydride is polymerised and reacted with allylamine to lead to an amide functionalised plasma polymer which can be heated at high temperature to get imide functional groups.

2. EXPERIMENTAL

2.1. Materials

The aluminium substrates was supplied by Pechiney (Voreppe, France). These samples were cut into pieces $90 \times 30 \times 0.5\,mm^3$ and they were cleaned by an argon plasma (100 W) for 2 min before plasma deposition.

EPDM (Buna AP 541) was provided by Bayer (Puteaux, France). Dicumyl peroxide (98% purity) from Aldrich, (3 phr, Lyon, France), was used as a crosslinking agent. EPDM sheets were previously moulded between Mylar® (DuPont de Nemours, Luxembourg) sheets under pressure (3 MPa at 90°C for 8 min) to obtain uncrosslinked plane films of $90 \times 30 \times 2\,mm^3$. A cotton cloth was added to limit the deformation of the elastomer during the peel test.

Briquettes of maleic anhydride (99.5% purity) were provided by Prolabo (Fontenay Sous Bois, France) and were used as received. Allylamine (99+%) was purchased from Aldrich and was used without any further purification.

2.2. Aluminum Surface Functionalisation

Maleic anhydride was ground into a fine powder and loaded into a stoppered glass gas delivery tube. Plasma polymerisation experiments were carried out in an electrodeless cylindrical glass reactor

(6 cm diameter, 680 cm^3 volume, base pressure of 5×10^{-4} mbar, and with a leak rate better than 1.0×10^{-10} kg/s) enclosed in a Faraday cage. The chamber was fitted with a gas inlet, a Pirani pressure gauge, a two-stage rotary pump (Edwards, Gennevilliers, France) connected to a liquid nitrogen cold trap and an externally wound copper coil (4 mm diameter, 5 turns). All joints were grease-free. An L-C matching network (Dressler, Lumbin, France, VM 1500 W-ICP) was used to match the output impedance of a 13.56 MHz radio frequency power supply (Dressler, Cesar 133) to the partially ionised gas load by minimizing the standing wave ratio of the transmitted power. During electrical pulsing, the pulse shape was monitored with an oscilloscope and the average power, $<P>$, delivered to the system was calculated using the following expression: $<P>=P_p\,[t_{on}/(t_{on}+t_{off})]$, where P_p is the average continuous wave power output and $t_{on}/(t_{on}+t_{off})$ is defined as the duty cycle.

Prior to each experiment, the reactor was cleaned by scrubbing with detergent, rinsing in propane-2-ol, oven drying, followed by a 30 min high-power (60 W) air plasma treatment. The system was then vented to air and the aluminium substrates were placed into the centre of the chamber followed by evacuation back down to base pressure. Subsequently, maleic anhydride vapour was introduced into the reaction chamber at a constant pressure of 0.2 mbar and with a flow rate of approximately 1.6×10^{-9} kg/s. At this stage, the plasma was ignited and run for 30 min. The optimum deposition conditions correspond to: power output = 5 W, pulse on-time = 25 μs, and off-time = 1200 μs. These parameters were previously optimised on the basis of a full factorial design and a central composite approach to get maximum maleic anhydride concentration in the polymer coating [13]. Upon completion of deposition, the R.F. generator was switched off and the monomer feed allowed to continue to flow through the system for a further 2 min period prior to venting up to atmospheric pressure. Then, the maleic anhydride plasma polymer deposited films were reacted with allylamine. This was carried out under vacuum without exposure to air.

At this stage, timing of the surface functionalisation reaction started. Upon termination of exposure (2 hours), the allylamine reservoir was isolated and the whole apparatus pumped back down to the system base pressure. The alkene functionalised substrates were removed from the reactor and placed in an oven under vacuum at 120°C for 2 hours. The various steps of the aluminium treatment are summarized on Figure 1.

Thickness of the deposited films was estimated by ellipsometry. Ellipsometry measurements were performed on a phase modulation Multiskop from OPTREL GBR (Berlin, Germany) at 632.8 nm (HeNe

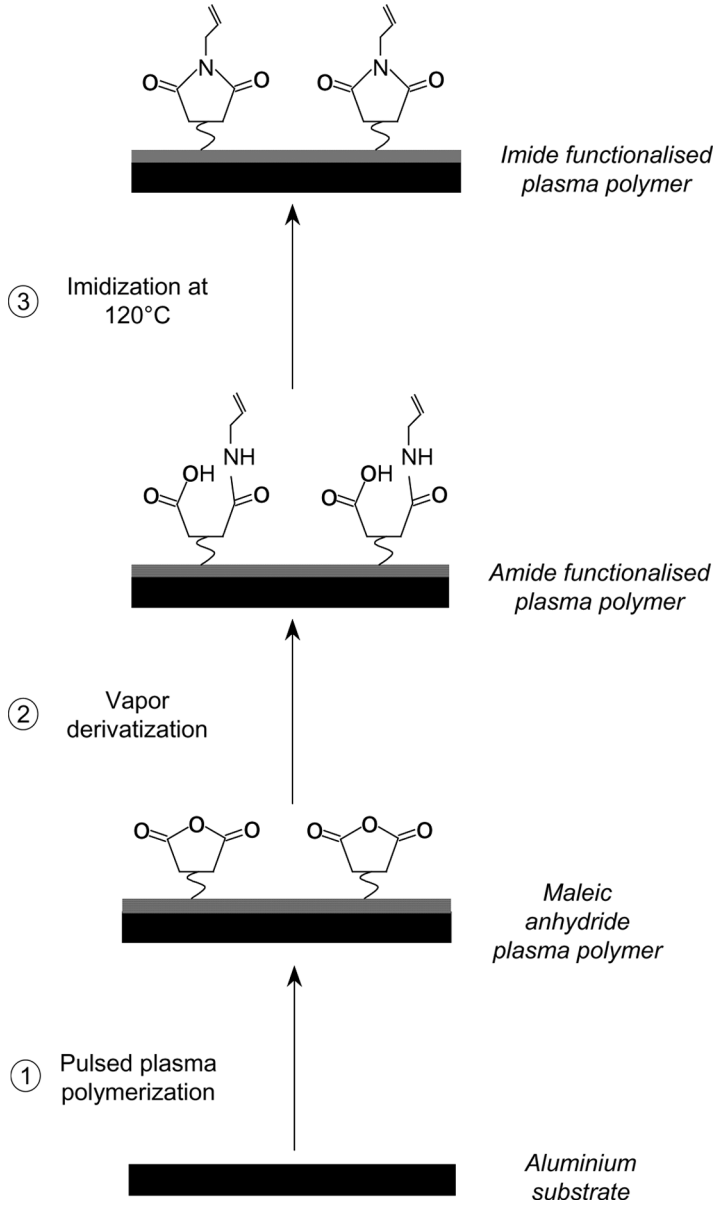

FIGURE 1 Various steps of treatment of the aluminium substrates: (1) maleic anhydride plasma polymer, (2) amide functionalisation and, (3) imide functionalisation.

laser). The cross section of the laser beam is about 1 mm^2. Measurements in air were performed at different positions (at least five) of the samples in order to check the quality of the films.

2.3. T-Peel Strength

Adhesive joints using alkene functionalised aluminium substrate ($90 \times 30 \times 0.5\,mm^3$) and EPDM sheet ($90 \times 30 \times 2\,mm^3$) were obtained by assembling the sheets at 170°C for 40 min under 3 MPa. During that step, the EPDM crosslinking occurred leading to a network with a molecular weight between crosslinks equal to 4380 g/mol as determined by swelling measurements in cyclohexane.

An INSTRON 4505 dynamometer (Instron, Guyancourt, France) was used to perform the 180° peel test (peel rate = 5 and 20 mm/min). min). Peel force was measured at room temperature and 72 hours after joint formation. Maleic anhydride plasma polymer functionalised aluminium substrates/EPDM joints were used as references. At least three replicates for each adhesive joint were carried out. The error was less than 1 J/m^2. The failed surfaces obtained after the peel test were analysed using infrared spectroscopy, XPS spectroscopy, contact angle measurements, and SEM images to accurately assess the locus of failure in the joints.

2.4. Surface Analysis

2.4.1. FTIR Spectroscopy

Polarization modulated-infrared reflection absorption spectroscopy (PM-IRRAS) is a reflection technique using high angle of incidence well suited to the study of thin film deposited on metals with a high refractive index [14]. PM-IRRAS spectra on the aluminium substrate were recorded with a Bruker IFS 66/S infrared spectrometer (Bruker, Wissembourg, France) equipped with a PMA 37 polarization modulation module and with a nitrogen cooled MCT detector. The infrared beam was p-polarized with a ZnSe wire grid polariser (Specac, Kent, UK) before passing through a photoelastic modulator (Hinds Instruments, Hillsboro, OR, USA). A total of 250 scans were collected for each measurement at an angle of incidence of 82.5° with respect to the surface normal.

For the EPDM surface after peeling, ATR spectra with a crystal of germanium was considered which corresponds to an analysed thickness of about 1 to 2 μm depending on the wavenumber considered. Mono-reflection technique was used with a germanium MIRacle™ from Pike Technologies Inc. (Madison, WI, USA).

2.4.2. X-Ray Photoelectron Spectroscopy (XPS)

XPS analysis of the functionalised surfaces utilized a LEYBOLD LHS11 instrument (Leybold, Germany) equipped with an non-monochromatised Mg $K\alpha_{1,2}$ X-ray source (1253.6 eV) and a concentric hemispherical analyser. Photo-emitted electrons were collected at a take-off angle of 90° from the substrate, with electron detection in the constant analyser energy mode (CAE, pass energy = 20 eV). Core level spectra were fitted using a Gaussian-Lorentzian product function with equal full-width-at-half-maximum (FWHM) using CASAXPS software (Casa software, Teignmouth, UK). The Gaussian/Lorentzian ratio was taken as 30% for all peaks. The binding energy of the CHx component in the C1s region was set to 285.0 eV and used for referencing. Instrumental sensitivity (multiplication) factors for C(1s):O(1s):N(1s):Al(2p) were taken, respectively, as equal to 1.0:2.86:1.77:0.57.

2.4.3. Contact Angle Measurements

Sessile drop contact angle measurements were carried out using a contact angle measuring system G2 from KRÜSS (Hamburg, Germany) with 3-μl high-purity water drops. The droplet was then enlarged while measuring the contact angle to obtain the advancing contact angle. The volume of the drop was differentially incremented until the contact line was observed to advance. The contact angle obtained just before the meniscus moves was measured as the advancing contact angle. Likewise, receding contact angle values were determined by withdrawing liquid from the droplet.

2.4.4. Scanning Electron Microscopy (SEM)

The SEM observations were performed onto a FEI environmental microscope (Quanta 400 model, FEI, Limeil Brevannes, France) working at 30 keV. The films were observed using the low vacuum mode in order to avoid artifacts due to the metallisation of the samples. The observations were performed in the presence of water vapour at a pressure of 1 Torr in the microscope chamber. No surface preparation of the samples was needed for observations in such conditions.

3. RESULTS AND DISCUSSION

3.1. Alkene Functionalised Plasma Polymer Deposited onto Aluminium Surfaces

The deposited maleic anhydride pulsed plasma film thickness on silicon wafer was estimated by ellipsometry to be 20 nm ± 2 nm. When the plasma polymer coating thin film was deposited onto an

aluminium substrate XPS analysis indicated five types of carbon functionality in the C(1s) envelope: hydrocarbon ($\underline{C}H_x \sim 285.0$ eV), carbon singly bonded to an anhydride group ($\underline{C}-C(O)=O- \sim 285.7$ eV), carbon singly bonded to oxygen ($-\underline{C}-O \sim 286.6$ eV), carbon doubly bonded to oxygen ($O-\underline{C}-O/-\underline{C}=O \sim 287.9$ eV), and anhydride or carboxylic acid groups ($O=\underline{C}-O-\underline{C}=O$ or $HO-\underline{C}=O \sim 289.4$ eV) (Figure 2a). The presence of anhydride groups is confirmed by the presence of two peaks in the high resolution spectra of the O (1 s) corresponding to oxygen doubly bonded to carbon ($-C=\underline{O}$) at 532.5 eV and oxygen singly bonded to carbon ($O=C-\underline{O}-C=O$) at 533.8 eV. These results are in agreement with previously published data [13,15,16]. Complete coverage of

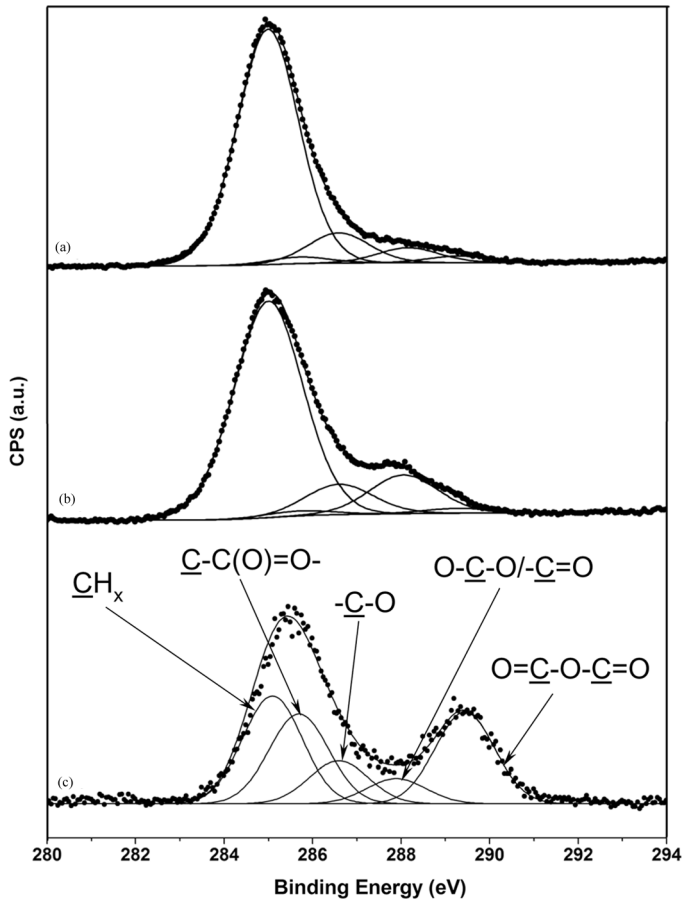

FIGURE 2 C(1s) XPS envelopes of (a) maleic anhydride pulsed plasma polymer; (b) followed by allylamine exposure; (c) then heating at 120°C.

the underlying aluminium substrate was confirmed by the absence of any Al(2p) signal showing through. Infrared analysis of the deposited maleic anhydride pulsed plasma polymer films confirmed a high degree of anhydride group incorporation as shown in Figure 3a.

When considering thicker superficial layers as analysed by infrared spectroscopy, the following absorption features of cyclic anhydride groups were identified: asymmetric and symmetric C=O stretching (1860 cm^{-1} and 1796 cm^{-1}), cyclic conjugated anhydride group stretching (1241–1196 cm^{-1}), C−O−C stretching vibrations (1097–1062 cm^{-1}), and cyclic unconjugated anhydride group stretching (964–906 cm^{-1}).

Reaction of allylamine (Figure 3b) in the gaseous phase with the deposited maleic anhydride pulsed plasma polymer layer resulted in a ring opening of the cyclic anhydride to yield the corresponding amide (amide I at 1658 cm^{-1} and amide II at 1550–1510 cm^{-1}), and carboxylic acid stretching (1716 cm^{-1}) infrared absorbances as shown in Figure 3c.

A corresponding change in the elemental XPS composition was found at the plasma polymer surface following exposure to allylamine vapour as indicated by the introduction of 9% of nitrogen in the elemental composition and a decrease of the oxygen content (Table 1). An accompanying change in the C(1s) envelope was also evident as can be observed in Figure 2b: hydrocarbon ($\underline{C}H_x \sim 285.0$ eV), carbon singly bonded to an amide/carboxylic acid group ($\underline{C}H_2C(O)NHR/\underline{C}H_2C-(O)OH \sim 285.6$ eV), carbon singly bonded to oxygen ($\underline{C}-O \sim 286.4$ eV), amide groups (RNH−C=O ~ 287.9 eV), and anhydride/carboxylic acid/carbonyl groups ($O=\underline{C}-O-\underline{C}=O/\underline{C}(O)OH/\underline{C}(O)O^-$ ~289.4 eV). The peak at 289.4 eV readily drops in intensity indicating a decrease in the concentration of the anhydride/carboxylic acid/carcarbonyl carboxylate groups at the surface. However, according to the scheme depicted in Figure 1, we expected that this peak would have the same intensity as the peak at 287.9 eV, corresponding to the amide groups. In other words, the intensity ratio of these peaks should be equal to 1. After the aminolysis reaction the value of this ratio is 0.13 showing that the reaction between carboxylic acid and amino groups after the maleic anhydride ring opening is effective but leads also to amide linkages. Two types of nitrogen functionality were identified in the N(1s) spectrum (Figure 4a): a major component at 399.8 eV corresponding to C(=O)−N(H)−C groups and a minor component at 401.5 eV corresponding to $C-NH_3^+$ groups due to acid-base interactions [17].

Heating these plasma polymer treated aluminium substrates to 120°C gave rise to the formation of cyclic imide groups as seen by the drop in intensity of strong amide and C=O acid bands in FTIR

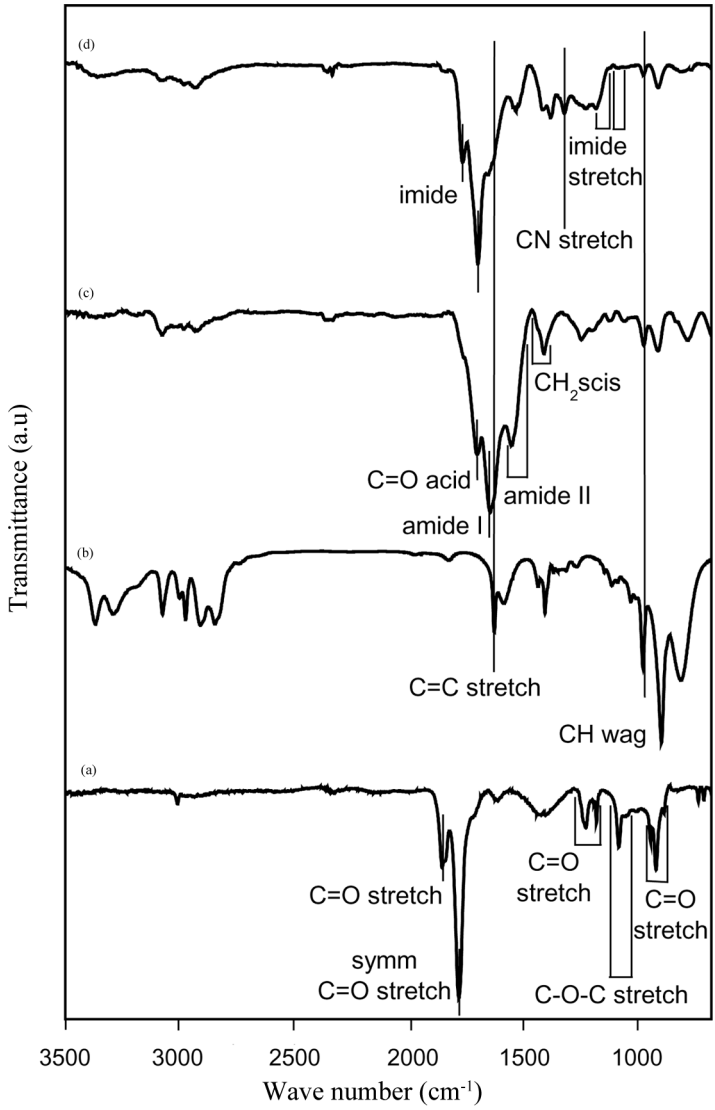

FIGURE 3 PM-IRRAS spectra of (a) maleic anhydride pulsed plasma polymer (c) allylamine-derivatised maleic anhydride pulsed plasma polymer and (d) allylamine-derivatised maleic anhydride pulsed plasma polymer after heating at 120°C for 2 hours. Spectrum, (b) is the transmission infrared spectrum of allylamine.

TABLE 1 XPS and Contact Angle Analysis of Substrates and Derivatised Plasma Polymer Thin Films

	XPS				Contact angles (°)
	%C	%O	%N	%Al	Adv/Rec
EPDM	95.6	4.4	0	0	$103^\circ \pm 2^\circ/45^\circ \pm 2^\circ$
Aluminium coated with					
Maleic anhydride plasma polymer	64	36	0	0	$61^\circ \pm 2^\circ/<10^\circ$
Amide functionalised plasma polymer	72	18	9	0	$12^\circ \pm 2^\circ/<10^\circ$
Imide functionalised plasma polymer	77	15	8	0	$60^\circ \pm 2^\circ/<10^\circ$

analysis, whilst two imide stretching vibration bands appear at 1775 cm^{-1} and 1710 cm^{-1} as reported in Figure 3d. Other new features include CN stretching vibrations at 1337 cm^{-1} and two new bands at 1210–1140 cm^{-1} characteristic of CNC symmetric and asymmetric stretching (imide stretching), respectively. The formation of cyclic imide appeared to be restricted to the near-surface region as background

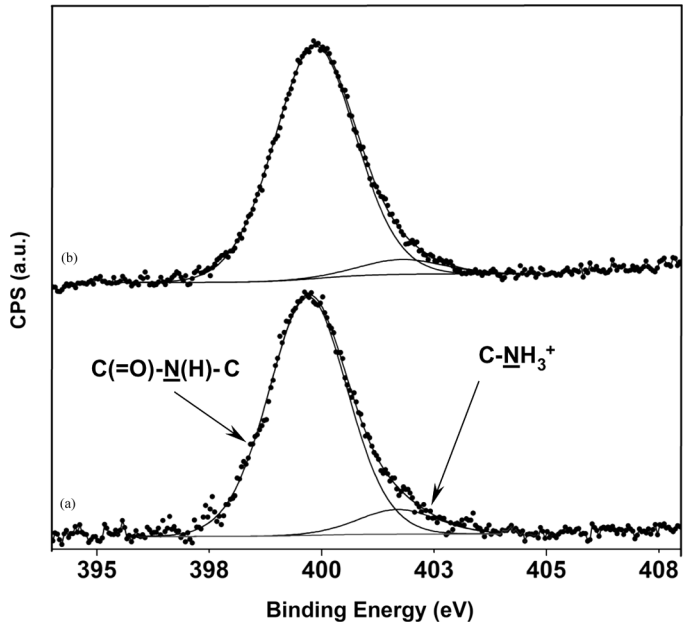

FIGURE 4 N(1s) XPS envelopes of maleic anhydride pulsed plasma polymer followed by (a) allylamine exposure and (b) after heating at 120°C.

amide infrared features remain. However, no changes were observed in the C=C stretching (1638 cm^{-1}) and the CH wagging (995 cm^{-1}) bands associated with the terminal alkene groups. The C(1s) envelope in XPS analysis indicates also chemical changes in the plasma polymer thin film: hydrocarbon ($\underline{C}H_x \sim 285.0$ eV), carbon singly bonded to an amide/carboxylic acid group ($\underline{C}H_2C(O)NHR/CH_2C-(O)OH \sim 285.6$ eV), carbon singly bonded to oxygen ($\underline{C}-O \sim 286.6$ eV), cyclic imide groups ($O=C-N(R)-\underline{C}=O \sim 288.2$ eV), and anhydride/carboxylic acid/carbonyl carboxylate groups ($O=\underline{C}-O-\underline{C}=O/\underline{C}(O)OH/\underline{C}(O)O^- \sim 289.3$ eV). A shift of the peak characteristic of the amide groups to the higher binding energy (288.2 eV) indicates imide linkages. Whilst the peak corresponding to the anhydride/carboxylic acid/carbonyl groups remains, showing that the cyclic imide formation is not effective through the entire polymer thin film. XPS analysis shows a small decrease in the total N(1s) signal due to removal of acid-base interactions accompanied by a decrease in intensity of the component at 401.5 eV, corresponding to $C-NH_3^+$ (Figure 4b).

Advancing contact angles measurements taken at each stage of this reaction scheme were found to be consistent with the aforementioned description (Table 1). A change in advancing water contact angle (61° to 12°) occurred upon reaction of allylamine with maleic anhydride plasma polymer surface indicating increased interactions with water. Imidisation produced again an increase in contact angle (60°) due to the elimination of surface carboxylic acid groups and removal of acid-base interactions [15]. The corresponding receding contact angle values are found to be less than 10°. A negligible change in thickness of the plasma polymer layer occurred during this 3-step reaction scheme.

3.2. Surface Characterization of EPDM Sheets

The FTIR reference spectrum of the EPDM networks is in accordance with previously published data [18] (Figure 5). The bands originating from the symmetric and asymmetric stretching vibrations of the methyl and methylene groups (ν_{as}, ν_s, (CH_3)) are, respectively, centred at 2950 cm^{-1} and 2800 cm^{-1}. The stretching vibrations of the C–H groups of propylene are localised at 1154 cm^{-1}, 1375 cm^{-1}, 1460 cm^{-1}, and 2723 cm^{-1}. The bending vibrations (δ(CH)) of the C–H groups of the double bond can be observed at 725 cm^{-1} and 808 cm^{-1}.

XPS analysis indicates only two types of carbon functionality in the C(1s) envelope: hydrocarbon ($\underline{C}H_x \sim 285.0$ V) and carbon singly bonded to oxygen ($-\underline{C}-O \sim 286.6$ V) as given in Figure 6a. The O(1s)

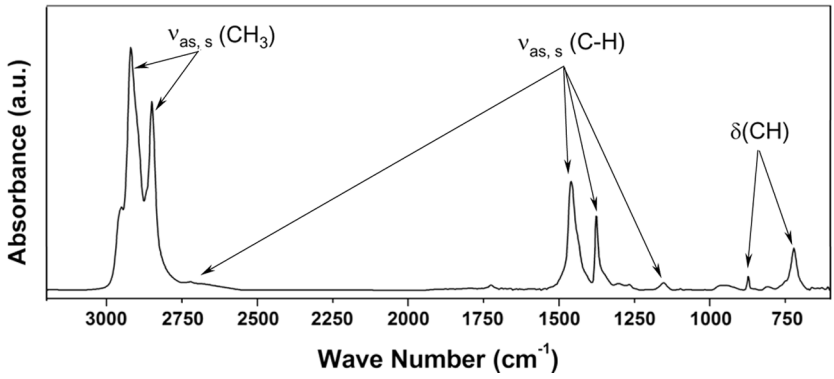

FIGURE 5 ATR-FTIR spectra of the EPDM surface.

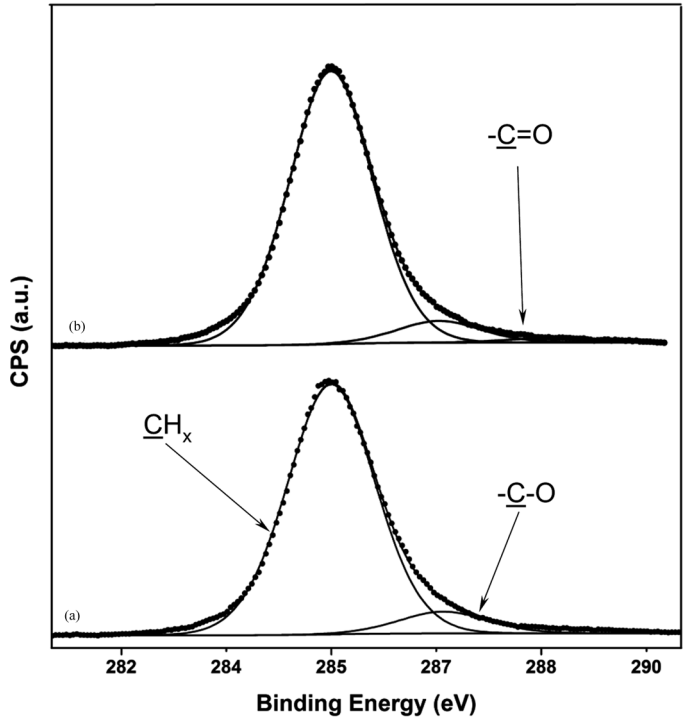

FIGURE 6 C(1s) XPS envelopes of EPDM surface (a) before peeling and (b) after peeling.

envelope presents only one peak centered at 532.4 eV corresponding to −C−O− (Figure 7a).

Finally, the water contact angle value of 103° indicates that the surface of the EPDM is hydrophobic (Table 1).

3.3. Peel Test Measurements

Alkene functionalised aluminium substrate/EPDM joints were obtained by assembling the sheets at 170°C for 40 min under 3 MPa. Figure 8 reports the peel force as a function of the peeled length for the imide treated aluminium substrate/EPDM joints for the two peel rates. The same values are obtained for joints made with amide treated aluminium. It can be observed that there is at least a ten-fold increase of the peel force compared with the aluminium substrate coated with the maleic anhydride plasma polymer/EPDM joint; see reference spectra on the same figure. The presence of the double bonds in the plasma polymer leads then to the reaction of the double

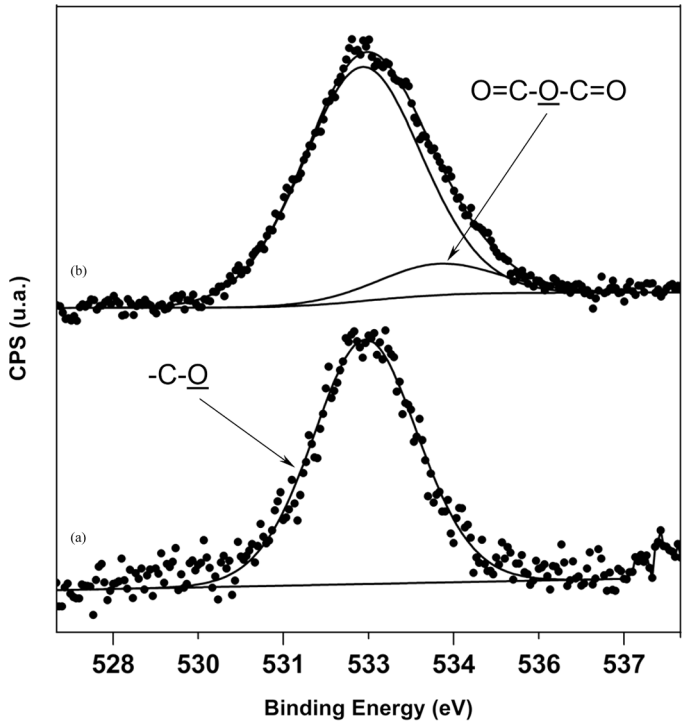

FIGURE 7 O(1s) XPS envelopes of EPDM surface (a) before peeling and (b) after peeling.

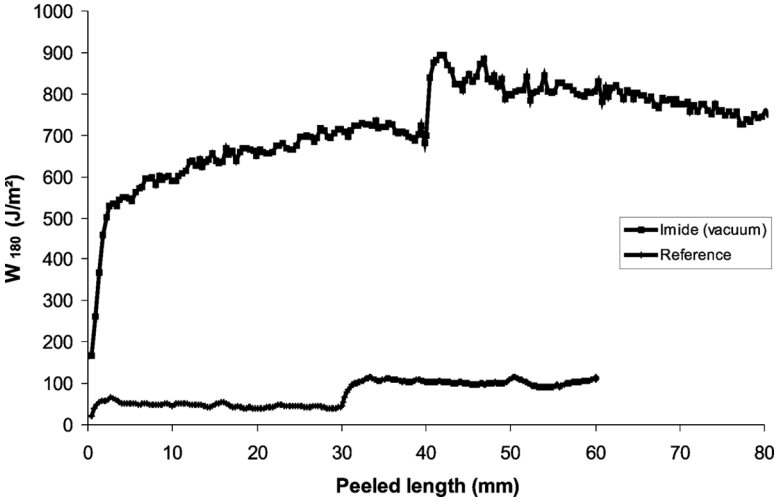

FIGURE 8 Peel force as a function of peeled length for imide treated aluminium substrate/EPDM.

bonds during crosslinking with peroxide and formation of covalent bonds at the interface between the elastomer and the treated metal which increase the interfacial strength. Adhesion strength is higher than cohesive strength. Indeed, the tear strength (trouser test piece) of EPDM at the same degree of crosslinking measured at 5 mm/min is equal to about 600–700 J/m^2 [19]. After peeling a thin layer of elastomer remains on the aluminium substrate which corresponds to an apparently cohesive failure occurring in the elastomer phase that we need to characterize more accurately.

3.4. Surface Analysis After Peel Test

The loci of failure of the adhesive joints were assessed by analysing the failed surfaces after the peel test using PM-IRRAS spectroscopy on the aluminium substrates, XPS spectroscopy, contact angle measurements, and SEM photographs. The locus of failure is different in the adhesive joint according to the presence or not of alkene functionalities. No changes were observed after peeling the joints produced with maleic anhydride functionalised aluminium substrates and, thus, an adhesive failure is obtained (results not shown). However, when the joint was obtained with alkene functionalised aluminium substrates, surface analysis was different before and after peeling indicating a mixed failure in both the EPDM phase and plasma polymer coating.

SEM images of the aluminium substrate after peeling reveal an heterogeneous surface composed of polymer islands and bare aluminium substrate (Figure 9). Whilst SEM images of EPDM show no change before and after peeling, a mixed failure on the aluminium side is observed.

Table 2 reports advancing and receding contact angles of water on crosslinked EPDM and treated aluminium substrate after peeling. These values can be compared with that given in Table 1 for the same substrates before assembly. It is clearly seen that the contact angles on the metal substrate after peeling get close to that of the crosslinked EPDM confirming the presence of elastomer on the metal substrate.

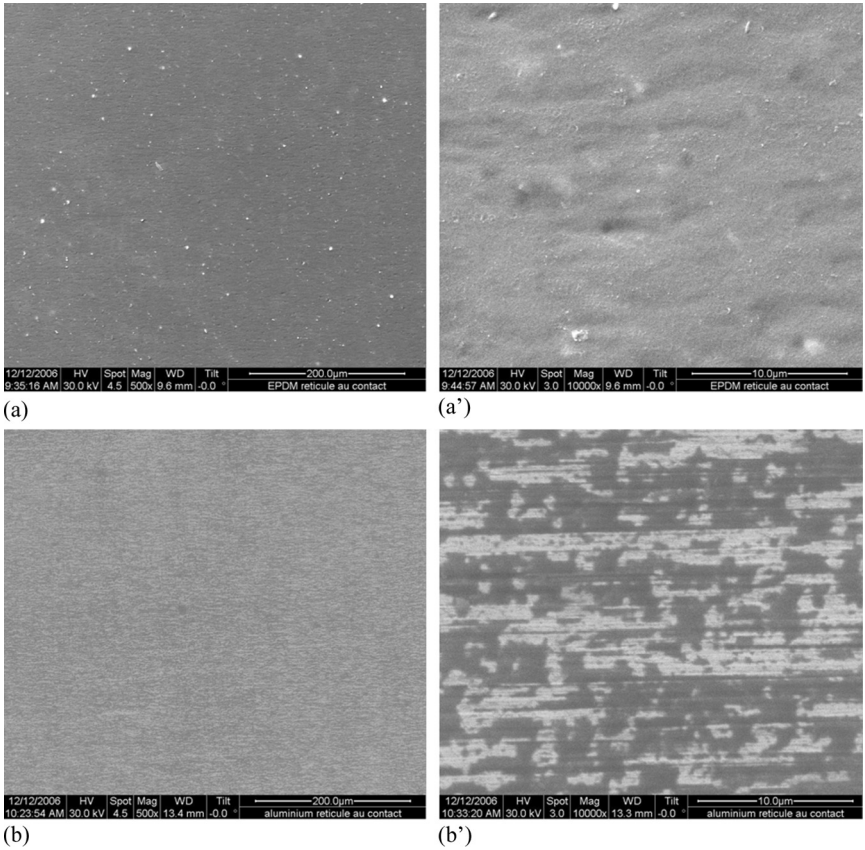

FIGURE 9 SEM images at two different scales (magnification 500 and 10000) of surface after peeling: EPDM (a and a') and imide treated aluminium substrate (b and b').

TABLE 2 XPS and Contact Angle Analysis of the Substrates After Peeling

	XPS				Contact angles (°)
	% C	% O	% N	% Al	Adv/Rec
EPDM	95.7	3.1	1.2	0	$103° \pm 2°/45° \pm 2°$
Imide functionalised aluminium	73.0	15.7	2.3	9.0	$100° \pm 2°/35° \pm 2°$

Different peaks in the PM-IRRAS spectra of the aluminium substrate allow one to differentiate the EPDM and the alkene functionalised plasma polymer. The most typical bands associated with the alkene functionalised plasma polymer are imide bands at 1775 cm^{-1} and 1710 cm^{-1} and the characteristic bands of amide I at 1658 cm^{-1} and amide II at 1550–1510 cm^{-1}. The strong fingerprint spectral features associated with the EPDM are observed: symmetric and asymmetric stretching vibrations of methyl and methylene groups at 2950 cm^{-1}, 2800 cm^{-1}, and 2723 cm^{-1} and the band at 1460 cm^{-1} belonging to the stretching vibration of the C–H groups of propylene. Comparing Figures 5 and 10a, no changes in the characteristics infrared absorption features of EPDM substrate appear before and after the peel test. However, ATR analysis may not be sensitive enough if other functional groups were present in small amounts due to the thickness of the rubber layer that is probed by this technique which is only about 1–2 μm.

PM-IRRAS analysis of the aluminium substrate indicates that imide functionalised groups remain onto the surface, Figure 10b. There are also the characteristic bands of amide functionalised groups showing that all amide groups were not transformed during the treatment at high temperature. But the strong fingerprint spectral features associated with the EPDM are also identified at 2950 cm^{-1}, 2800 cm^{-1}, 2723 cm^{-1}, and 1460 cm^{-1}.

Table 2 reports the surface composition as obtained by XPS analysis on both substrates after peeling. Aluminium appears clearly on the functionalised aluminium substrate after peeling, revealing that some plasma polymer was transferred to the EPDM substrate; no aluminium peak was observed after the alkene plasma treatment. This was confirmed by the presence of nitrogen on the EPDM side also shown in Table 2.

XPS spectra of the alkene functionalised aluminium substrate after peeling are not shown because they are very comparable with that shown on Figure 2. The decomposition of the corresponding

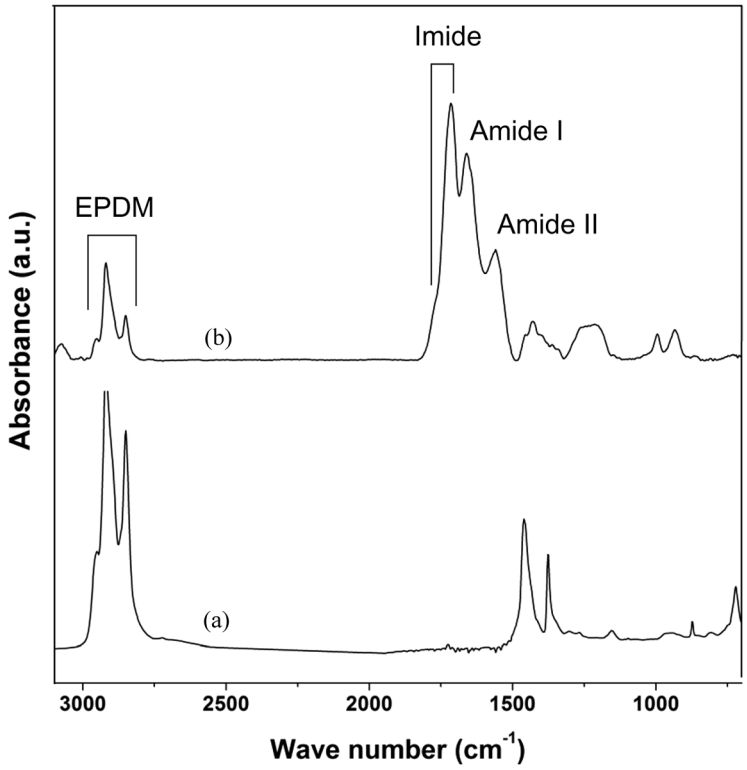

FIGURE 10 (a) ATR-FTIR spectra of the EPDM surface after peeling and (b) PM-IRRAS spectrum of imide treated aluminium substrate after peeling.

C(1s) envelope indicates (Table 3) five types of carbon functionalities as in functionalised aluminium substrate before contact with EPDM: hydrocarbon ($\underline{C}H_x \sim 285.0$ eV), carbon singly bonded to an amide/

TABLE 3 Decomposition of the C(1s) XPS Envelope of the Alkene Functionalised Aluminium After the Peel Test

	CH_x	$CH_2C(O)NHR$/ $CH_2C-(O)OH$	C–O	RNH–C=O	O=C–O–C=O/ C(O)OH/ $C(O)O^-$
Binding energy (eV)	~285	~285.7	~286.6	~287.9	~289.4
Atomic concentration (%)					
before peeling	80.1	2.2	10.3	5.2	2.2
after peeling	83.2	2.1	9.3	3.2	2.2

carboxylic acid groups ($\underline{C}H_2C(O)NHR/CH_2C-(O)OH \sim 285.7$ eV), carbon singly bonded to oxygen ($\underline{C}-O \sim 286.6$ eV), amide groups (RNH–$\underline{C}$=O ~ 287.9 eV), and anhydride/carboxylic acid/carboxylate groups ($\overline{O}$=$\underline{C}$–O–$\underline{C}$=O/$\underline{C}$(O)OH/$\underline{C}$(O)O^- ~ 289.4 eV). The corresponding O(1s) envelope also shows an increase of the concentration of the oxygen bonded to carbon: 95.9% of oxygen doubly bonded to carbon (–C–$\underline{O}$) at 532.2 eV and 4.1% of oxygen singly bonded to carbon (O=C–$\underline{O}$–C=O) at 533.8 eV. No change is observed in the N(1s) envelope.

Results obtained by the three techniques show that part of the failure occurs very close to the interface and part of it occurs close to the aluminium substrate. Moreover, the presence of three types of carbon functionality in the C(1s) envelope on the EPDM sheet after peeling is detected: 91.25% of hydrocarbon ($\underline{C}H_x \sim 285.0$ eV), 7.24% of carbon singly bonded to oxygen (–$\underline{C}$–O ~ 286.6 eV), and 1.5% of carbon doubly bonded to oxygen (–$\underline{C}$=O ~ 288.1 eV), Figure 6b. The signal at 288.1 eV is very close to the signal analysed on the alkene functionalised aluminium substrate at 287.9 eV before peeling, which is characteristic of the amide groups (RNH–C=O). The corresponding O(1s) envelope shows a shoulder at 533.7 eV which confirms the presence of anhydride groups remaining in the functionalised plasma polymer (see Section 3.1), Figure 7b. These results show that part of the failure also occurs in the alkene functionalised plasma polymer. It should be noticed that no peak corresponding to O–Al bonds (530.6 eV) is found which would mean that the most superficial layers of the aluminium substrate are modified by the plasma polymer treatment.

The elemental composition obtained by XPS is quite comparable with that of the plasma polymer, although the contact angle after peeling on the aluminium substrate clearly corresponds to that of the EPDM phase. A slight increase in the CH_x contribution seen in Table 3 after the peel test would correspond to a thin layer of EPDM left of the plasma polymer coating. If one roughly estimates that about 50% of the aluminium substrate is covered by EPDM on the basis of the SEM images, a layer of EPDM 4 nm thick that remains on the plasma polymer would correspond to a ratio of 83% of CH_x. This value is in good agreement with that reported in Table 3.

Therefore, it can be concluded that the thickness of the elastomer layer remaining on the metal substrate is very small if one considers that the water droplets in the contact angle measurements probe the outermost 5–10 Å; XPS analyses concern layers of about 5–8 nm with the 90° take-off angle used here.

An interphase resulting from the interactions between plasma polymerised acetylene films deposited onto steel which reacted with a

model vulcanised "rubber" was shown by Tsai *et al.* [20]. Delattre *et al.* [21] also showed a broadened interface between the vulcanised rubber in contact with a plasma polymerised thiophene film. The presence of such an interface with a gradient of crosslinking in the rubber phase cannot be excluded in the present case either.

4. CONCLUSION

The alkene plasma polymer functionalisation of aluminium substrates gives an increase in the adhesion of aluminium substrate to EPDM due to the formation of crosslinks between the elastomer and the coating during peroxide crosslinking of the elastomer. The peel strength value obtained is ten times as high as the peel strength measured with a maleic anhydride functionalised aluminium substrate. A mixed locus of failure (mainly cohesive in EPDM very close to the EPDM/plasma polymer interface) is obtained. This approach offers great flexibility in that the density of such alkene functionalities at the surface can be easily tailored by simply programming the pulsed plasma duty cycle [13].

REFERENCES

[1] Deruelle, M., Léger, L., and Tirrell, M., *Macromolecules* **28**, 7419–7428 (1995).
[2] Aradian, A., Raphaël, E., and de Gennes, P. G., *Macromolecules* **33**, 9444–9451 (2000).
[3] Ahagon, A. and Gent, A. N., *J. Polym. Sci., Part B Polym. Phys.* **13**, 1285–1300 (1975).
[4] Steen, M. L., Flory, W. C., Capps, N. E., and Fisher, E. R., *Chem Mat* **13**, 2749–2752 (2001).
[5] Morita, S. and Hattori, S., in *Plasma Deposition, Treatment and Etching of Polymers*, R. d'Agostino, (Ed.) (Academic Press, London, 1990).
[6] Hynes, A. and Badyal, J. P. S., *Chem. Mat.* **10**, 2177–2182 (1998).
[7] Kettle, A. P., Beck, A. J., O'Toole, L., Jones, F. R., and Short, R. D., *Composite Sci. Technol.* **57**, 1023–1032 (1997).
[8] Strobel, M., Lyons, C. S., and Mittal, K. L. (eds.), *Plasma Surface Modification of Polymers: Relevance to Adhesion* (VSP, Utrecht, The Netherlands, 1994) pp. 3–149.
[9] Tsai, Y. M., Boerio, F. J., and Kim, D. K., *J. Adhesion* **61**, 247–270 (1997).
[10] Kang, H. M., Chung, K. H., Kaang, S., and Yoon, T. H., *J. Adhesion Sci. Technol.* **15**(4), 467–481 (2001).
[11] Luo, S. and Van Ooij, W. J., *Rubber Chem. Technol.* **73**, 121–137 (1999).
[12] Krump, H., Hudec, I., Jasso, M., Dayss, E., and Luyt, A. S., *Appl. Surf. Sci.* **252**, 4264–4278 (2006).
[13] Siffer, F., Ponche, A., Fioux, P., Schultz, J., and Roucoules, V., *Analytica Chimica Acta* **539**, 289–299 (2005).
[14] Ishida, H., *Rubber Chem. Technol.* **60**(3), 497 (1987).

[15] Teare, D. O. H., Schofield, W. C. E., Roucoules, V., and Badyal, J. P. S., *Langmuir* **19**, 2398–2403 (2003).
[16] Roucoules, V., Fail, C. A., Schofield, W. C. E., Teare, D. O. H., and Badyal, J. P. S., *Langmuir* **21**, 1412–1415 (2005).
[17] Teare, D. O. H., Schofield, W. C. E., Garod, R. P., and Badyal, J. P. S., *Langmuir* **21**, 10818–10824 (2005).
[18] Morlat-Therias, S., Fanton, E., Tomer, N. S., Rana, S., Singh, R. P., and Gardette, J. L., *Polym. Degrad. Stab.* **91**, 3033–3039 (2006).
[19] Ruch, F., "Etude des Mécanismes d'Adhésion à l'Interface Élastomère/Élastomère," Ph.D. Thesis (06-Mulh-0857), University of Haute-Alsace, Mulhouse, France (January 1999).
[20] Tsai, Y. M., Boerio, F. J., and Kim, D. K., *J. Adhesion* **55**, 155–163 (1995).
[21] Delattre, J. L., d'Agostino, R., and Fracassi, F., *Appl. Surf. Sci.* **252**, 3912–3919 (2006).